LA-UR- 97-3482

Title: HIGH-RESOLUTION X-RAY SPECTROSCOPY OF HOLLOW ATOMS CREATED IN PLASMA HEATED BY SUBPICOSECOND LASER RADIATION

CONF-970706--

Author(s): A. Ya. Faenov, VNIIFTRI
J. Abdallah Jr., T-4
R. E. H. Clark, X-CI
J. Cohen, T-4
R. P. Johnson, P-24
G. A. Kyrala, P-24
A. I. Magunov, VNIIFTRI
T. A. Pikuz, VNIIFTRI
I. Yu. Skoblev, VNIIFTRI
M. D. Wilke, P-24

Submitted to: SPIE PROCEEDINGS CONFERENCE 97
SAN DIEGO, CA

Los Alamos
NATIONAL LABORATORY

Form No. 836
ST2629 10/91

DISCLAIMER

High-resolution X-ray spectroscopy of hollow atoms created in plasma heated by subpicosecond laser radiation

A.Ya. Faenov[a], J. Abdallah[b] Jr., R.E.H. Clark[b], J. Cohen[b], R.P. Johnson[b], G.A. Kyrala[b], A.I. Magunov[a], T.A. Pikuz[a], I.Yu. Skobelev[a], M.D. Wilke[b]

[a]Multicharged Ions Spectra Data Center of VNIIFTRI, Mendeleevo, Moscow region, 141570, Russia
[b]Los Alamos National Laboratory, P.O. Box 1663, Los Alamos, New Mexico 87545, USA

ABSTRACT

The investigations of ultrashort (0.4-0.6 ps) laser pulse radiation interaction with solid targets have been carried out. The Trident subpicosecond laser system was used for plasma creation. The X-ray plasma emission was investigated with the help of high-resolution spectrographs with spherically bent mica crystals. It is shown that when high contrast ultrashot laser pulses were used for plasma heating its emission spectra could not be explained in terms of commonly used theoretical models and transitions in so called "hollow atoms" must be taken into account for adequate description of plasma radiation.

Keywords: laser plasma, X-ray spectra, hollow atom, ultrashort laser pulses.

1. INTRODUCTION

The investigations of ultrashort (< 1 ps) laser pulse radiation interaction with gaseous and solid targets have had great activity during last years. The creation of more powerful laser facilities promises to give knowledge about fundamental properties of matter under critical conditions. On the other hand, it provides new solutions for different applications such as x-ray sources for medicine and biological chemistry, particle acceleration, ignition of nuclear reactions and some others (see, for example, Gibbon and Forster[1] and references inside). The results already received show the dominant role of processes that were of less importance for plasma in the case of nanosecond laser pulse duration[2-9]. The most complete information about these processes can be obtained from high-resolution x-ray spectroscopic measurements. The features of the line emission spectrum directly manifest the structure of the radiators and make it possible to evaluate the various processes of plasma creation.

Concerning the scenario of ultrashort pulse plasma production from solid state target, the laser radiation does not have time to create a long scale length below critical density plasma where the main part of the pulse energy is deposited by resonance absorption. In this case the energy of electromagnetic field transforms to hot electrons generated in a skin layer at or close to the surface. The mechanism of hot electron generation is the subject of experimental and theoretical studies and is not completely understood. The effective penetration of these hot electrons, of ten or more kilo electron volts in energy, to the below surface layers is followed by *K*-vacancy production. The secondary channel of the *K*-vacancy production is the photoionization by the hard and soft x-ray bremsstrahlung radiation produced by hot electrons. Thus, the emission from these cool plasma layers has to be formed mostly by inner shell vacancies, 'hollow', ions of different ionization stages. At present time the 'hollow' ions are of particular interest in the experiments with ion beam-surface interactions[10-12]. Many questions arise when the emission of ions, strongly driven by laser, is discussed. Their features become appropriate when ions are cool enough to suppress Doppler line broadening, and for the laser satellites to be observed in the emission spectra[13].

Our recent measurements of H-like and He-like ions x-ray line emission generated in the Trident laser 400-600 fs pulses interaction with solid targets from Na through Ti illustrates the drastic difference in these spectra compared with those for nanosecond pulses. The role of different processes in plasma formation can be elucidated from these experiments where a laser prepulse of 120 ps duration was combined with the main shot pulse in varying energy ratio. Focusing spectrometer with high spectral ($\lambda/\Delta\lambda$=10000) resolution was used to detect x-ray spectra near the He_α, He_β and Ly_α lines of different elements. The spatial resolution (Δx=10 mm) provides the detection of emission from the close-to-surface plasma, however the below-surface region could not be resolved separately.

We show that when high contrast ultrashort laser pulses were used for plasma heating, the emission spectra could not be explained in terms of commonly used theoretical models and transitions from the so called "hollow atoms" must be taken into account for the adequate description of the plasma radiation.

2. SETUP

A diagram of the optical layout of the laser beam from the output of the final amplifier to the target is given in fig.1. The chirped IR pulse passed through a polarizer which split off approximately 5% of the energy to a 2 inch Scientech optical calorimeter for incident energy determination. The beam then proceeded to the first grating, was reflected to the second grating, came to a periscope which returned the beam to the second grating at a higher level and finally back to the first grating for a second reflection. Following the final reflection on the first grating the pulse was fully compressed. The compressed beam was then picked off by a highly reflective mirror and directed to a 3 mm thick, Type I KDP doubling crystal. Leakage through the mirror was directed to a single shot autocorrelator for pulse width measurements. Following

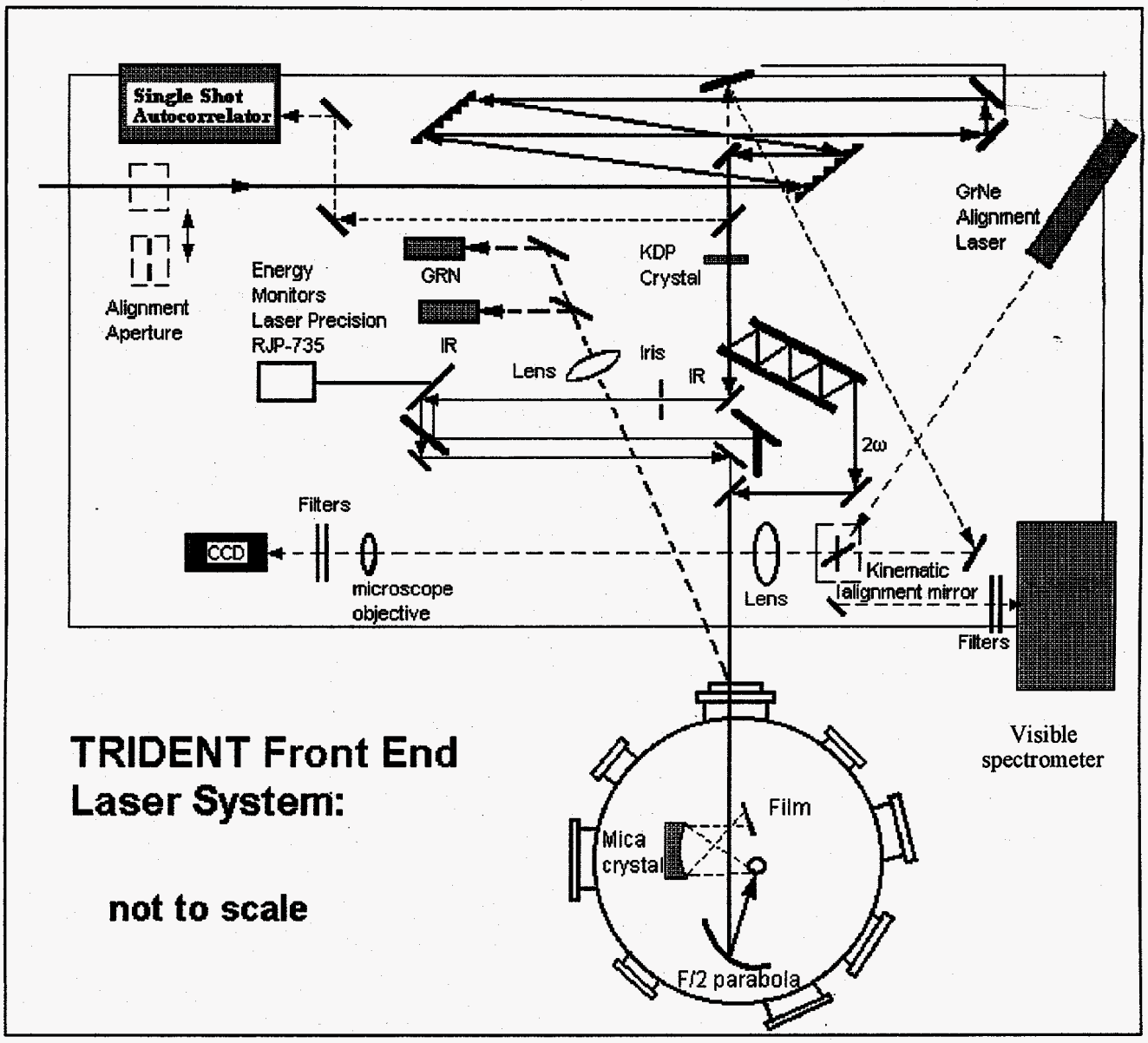

Fig.1 The scheme of TRIDENT laser system

the frequency doubling crystal the beam was directed to a green «rattle plate» - two parallel mirrors approximately 4 cm apart each having a reflectivity of greater than 99% for .527 μm light and a reflectivity of about 4% for 1.053 μm light. Mirror separation and angle were adjusted to result in 4 reflections on each mirror before the beam exited past the opposite edge. The beam was then directed to the target chamber via two 3 inch mirrors highly reflective for .527 μm light.

For 120 ps shots the 3 mm type I KDP crystal was replaced with a 15 mm thick type I KDP crystal providing about 50% conversion of the IR pulse to the green. All other optics remained the same.

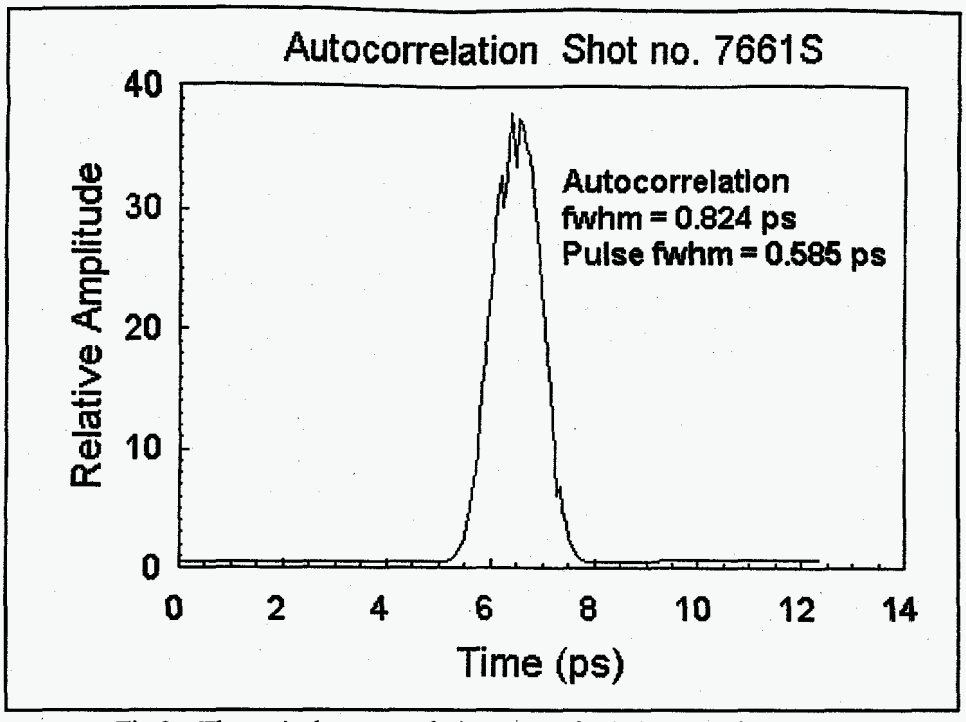

Fig.2a. The typical autocorrelation trace of subpicosecond IR pulse.

The beam path described included a total of ten reflections from «green only» mirrors, giving a total transmission of the second harmonic of > 90%, while IR transmission was reduced to $0.04^{10} = 10^{-14}$. IR leakage through the first «rattle plate» mirror was directed via highly reflective IR mirrors to a delay dogleg and then re-injected through the final green turning mirror into the target chamber to act as s prepulse for some shots. Both IR and green energy were monitored by monitoring the reflection from the uncoated calcium fluoride target chamber window.

A 40 mm diameter, 80 mm focal length off axis paraboloid mirror was used to focus the energy on to the target. This mirror was measured to have reflectivity of 98.5% at .527 μm and 2% at 1.053 μm.

Backscatter from the low power alignment beam was used to monitor the focal spot on the target. The backscattered light was recollimated by the focussing mirror, then transmitted by the optical system through an IR mirror as shown in figure 1. It was then refocused by a 1 mm focal length lens. The focal spot was then magnified with 10X microscope objective and recorded on a CCD video camera and framegrabber. During high power shots, a 2 inch aluminized mirror was placed in the backscattered beam which directed the energy to a backscatter spectrometer.

Energy Calibration

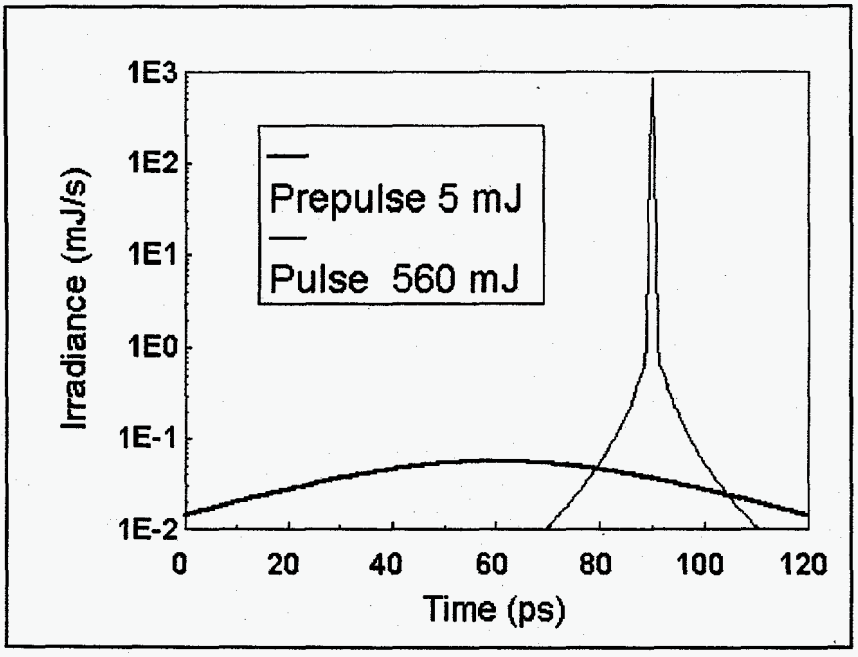

Fig. 2b. The relation between the main laser pulse and prepulse.

Energy calibrations were performed by placing a 2'' diameter Scientech calorimeter in the target chamber and collecting the entire full energy beam and calibrating the energy reflected from the uncoated target chamber window to the energy measured on the calorimeter. Two Laser Precision pyroelectric energy metres were used to measure IR and green energy separately. An IR reflector was used to direct the IR energy to the first detector that had a visible blocking filter in front. The green which passed through the IR mirror was then directed to a second defector with an IR blocking filter in place.

Green prepulse energy (120 ps) was calibrated after the experimental shots, by placing a Laser Precision pyroelectrinic energy metre directly in the beam in front of the target camber. Energy was then measured as a function

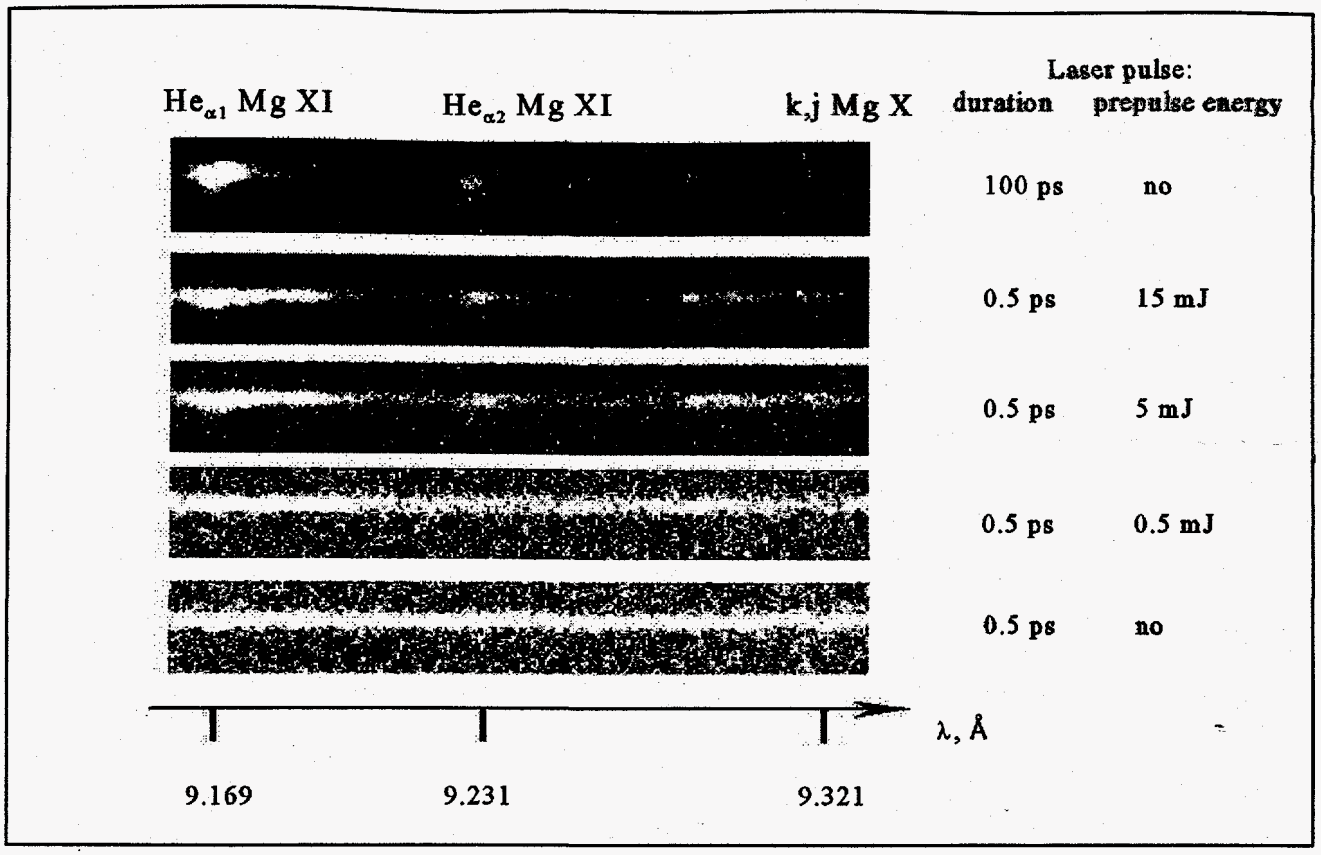

Fig.3a X-ray emission spectra of magnesium plasma heated by subnanosecond and subpicosecond laser pulses.

of PD4 diode setting. Since the 120 ps regenerative amplifier is quite stable, it is estimated that prepulse energy can be determined from the PD4 diode setting within 5%.

Temporal Pulse Measurements.

Two types of temporal pulse measurements were made during this experiment: (1) Sub-picosecond pulse width measurements were made with the single pulse autocorrelator, and (2) naturally occurring prepulse measurements were made in the nanosecond time scale with a Hamamatsu model R1328A vacuum photodiode and a Tektronix SCD 5000 oscilloscope.

Typical autocorrelation trace of subpicosecond IR pulse is shown in fig.2a for shot at high energy. There is some apparent pulse broadening which broadened the pulse to about 600 fs.

For some of the shots, intentional prepulse in the green were introduced (see Fig. 2b). 120 ps narrowband pulses from a second regenerative amplifier were coupled into the beam line in the front end. Stacker pulse number 10 was used, the peak of which was measured to precede the centre of the cpa pulse by approx 30 ps. To obtain 15 mJ in the prepulse on target, nearly 1 J of 120 ps was required. As the prepulse energy is increased it becomes apparent that the autocorrelator signals are affected by the prepulse.

The power ratio between the prepulse and the main pulse is given by
R = sl*FWHM1/(s2*FWHM2*T)
where sl = signal 1 = 1.2 V
s2 = signal 2 = 10 mV
FWHM1 = full width half max of diode signal = 100 ps
FWHM2 = full width half max of the actual pulse = .6 ps
T = transmission of the attenuating filter = .011

Substituting these values we obtain R = 1.8 x 10^6 for the IR contrast.It should be noted that in any case, an IR contrast of 10^6 would result in a second harmonic contrast of 10^{11}.

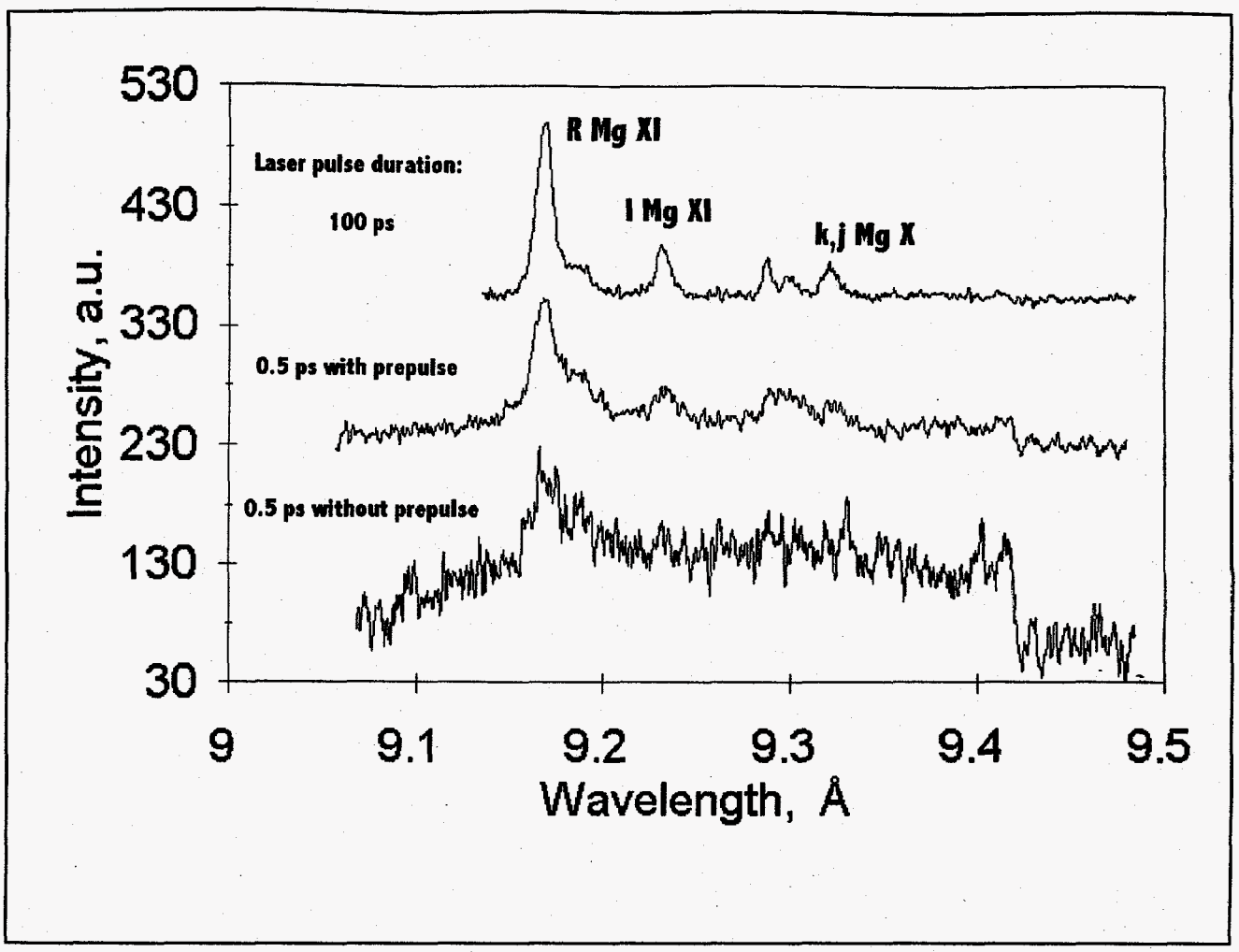

Fig.3b. Magnesium plasma emission in the vicinity of resonance line of He-like Mg XI.

Spatial beam measurements

Spatial profiles the low power RGA pulse and fully amplified pulses at about 500 mJ were measured by putting a retro reflecting uncoated BK7 wedged splitter in the beam inside the target chamber. The reflected light was directed to the CCD imaging system as shown in figure 1. Focussing on target was accomplished using an f/2 parabola. Assuming that the beam quality did not degrade when being focussed by the parabola, then spot size should be a factor of 12.5 smaller on target than measured with this system.

The spatial profile of the low power beam is nearly diffraction limited. As power was increased, however, more energy was scattered into low power wings around the central spot. For the low power beam approximately 70% of the energy is within a spot of 50 μm which translated to a beam diameter of about 4μm on target. On a high power shot 70% of the energy is contained within a 90 μm spot or 7μm on target.

A third measure of beam quality is to integrate the total exposure on the CCD and determine the amount of energy per pixel count and calculate the maximum energy density by knowing the maximum pixel and the pixel dimensions. Including the magnification of the optics pixel includes an area of 1.175 x 1.175 μm^2 . Using these numbers and the CCD exposure values it was calculated the peak fluence for the RGA pulse was 9.5 x 10^4 x Incident energy and the corresponding value for the high power pulse was 6,5 x 10^4 x Incident energy. This corresponds to only about a 30 % reduction in relative fluence for a given energy. The best estimate of fluence is then about 1 x 10^7 x Incident Energy in Joules/cm^2.

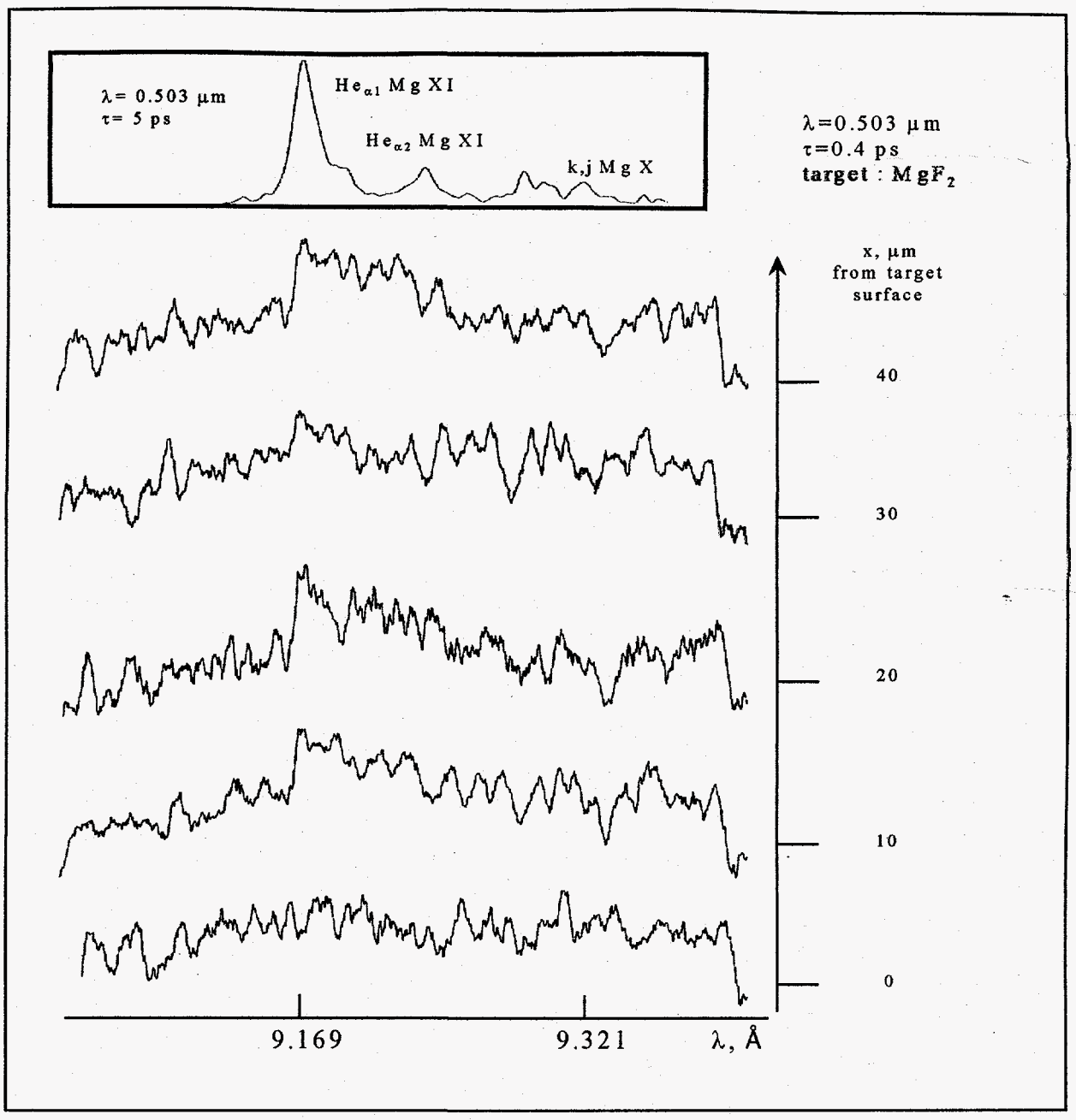

Fig.4.Spectra emitted by the regions of magnesium plasma placed at different distances from the target surface.

Most shots with «no prepulse» had peak intensities in the range of (0.5-1)x10^{19} W/cm^2. Power contrast between the main pulse and naturally occurring nanosecond time scale prepulse in the second harmonic was at least 10^{10} to 10^{11}.

For shots with a nominal «5 mJ» prepulse, the main pulse was probably partially split into two pulse approximately 1 ps fwhm separated by 1 ps, reducing peak irradiancy by about a factor of 3 to about 1.5 to 3 x 10^{18} W/cm^2. Prepulse energy was about 5 mJ on target, however, due to timing only about 70% of that energy reached the target before the main pulse. Prepulse energy was then about 3.5 mJ and Power contrast ratio was about 5 x 10^3 to 1 x 10^4.

For shots with a nominal «15 mJ» prepulse, the main pulse was split more completely, although peak irradiancy may not have degraded further (except for the fact that total energy was somewhat reduced on those shots) Prepulse energy was about 15 mJ. About 10 mJ reached the target before the main pulse providing a power contrast ratio of 1.5 x 10^3 to 3 x 10^3.

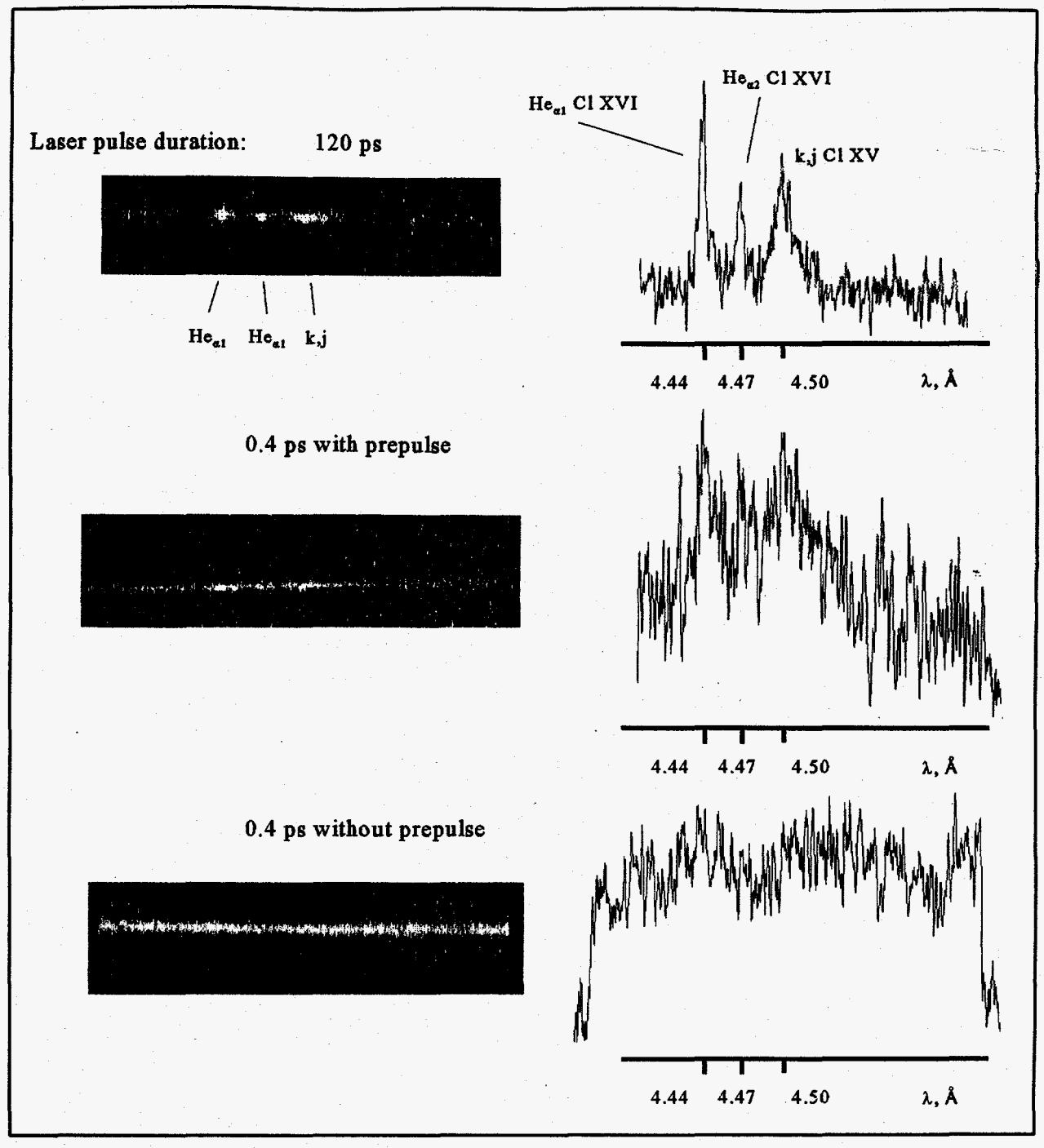

Fig.5. Spectra emitted by NaCl plasma heated by different laser pulses

Experiments with 120 ps shots ranged in energy from about 0.3 to 0. 5 J, providing a target irradiances of 2.5 to 4 x 10^{16} W/cm^2.

X-ray spectrographs

X-ray plasma emissions have been observed by means of spectrographs with a spherically bent mica crystals. Crystals with radii of curvature equal to 100, 150 and 186 mm have been used. The crystals, plasma and photographic film were placed according to the FSSR-1D and FSSR-2D schemes[2]. It allowed to have simultaneously high spectral ($\lambda/\Delta\lambda$=10000) and spatial (δx=10 μm) resolutions.

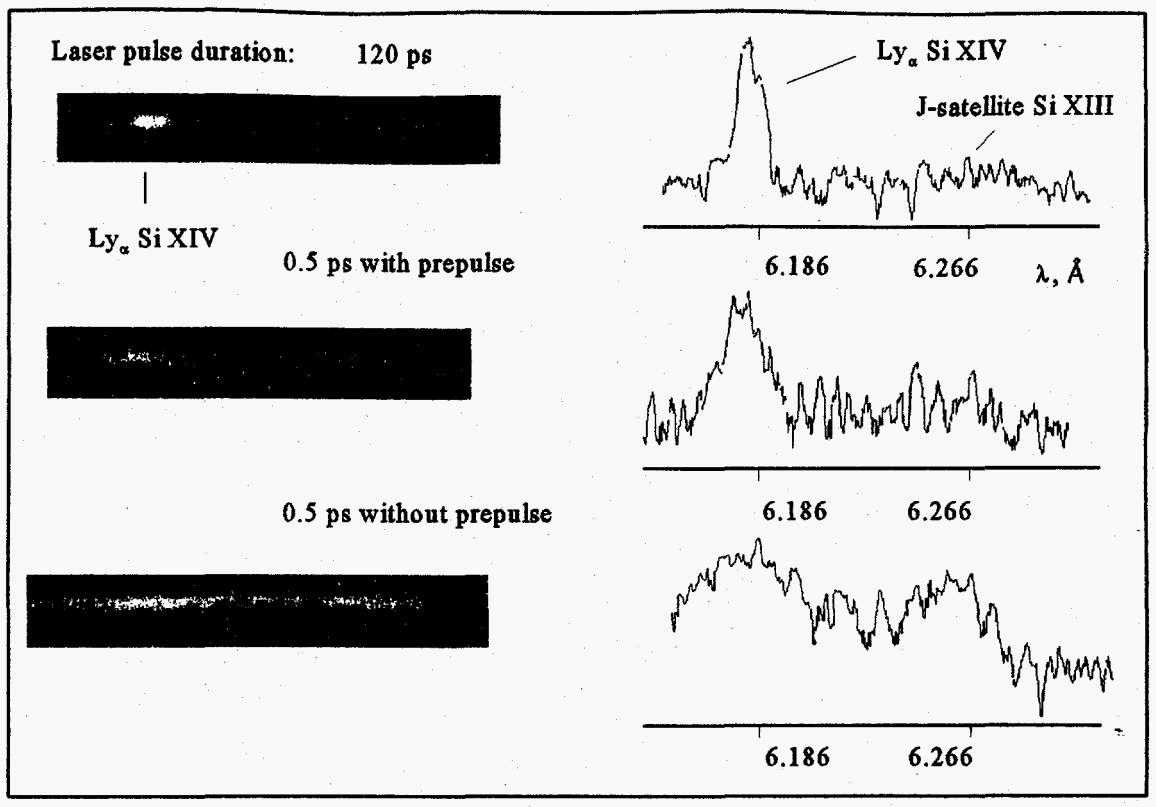

Fig.8. H-like Si XIV emission for different methods of plasma creation.

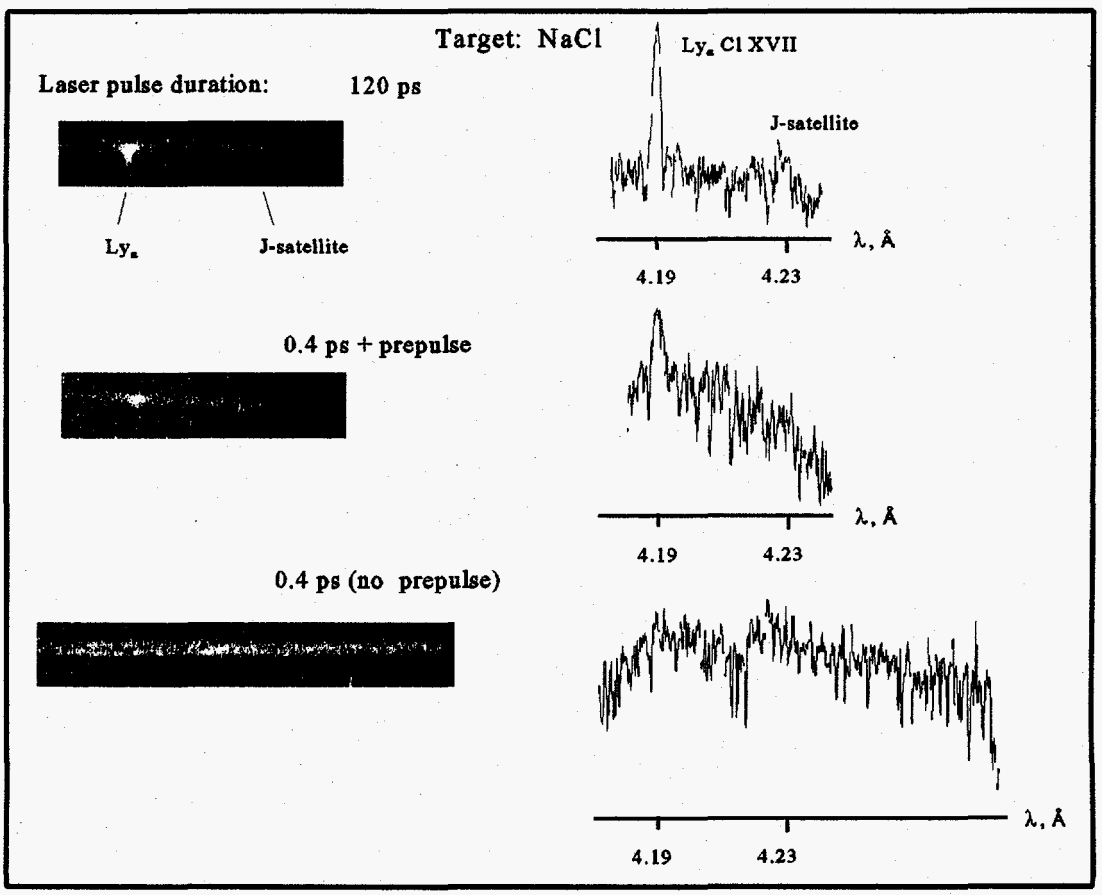

Fig.9. Spectra of chlorine laser-produced plasma in the vicinity of H-like Cl XVII resonance line.

3.RESULTS AND DISCUSSION

We have investigated x-ray plasma radiations in the spectral regions near resonance lines of H-like (Si XIV, Cl XVII) and He-like (Mg XI, Si XIII, Cl XVI, Ti XXI) ions. The results obtained are presented in figures 3-9.

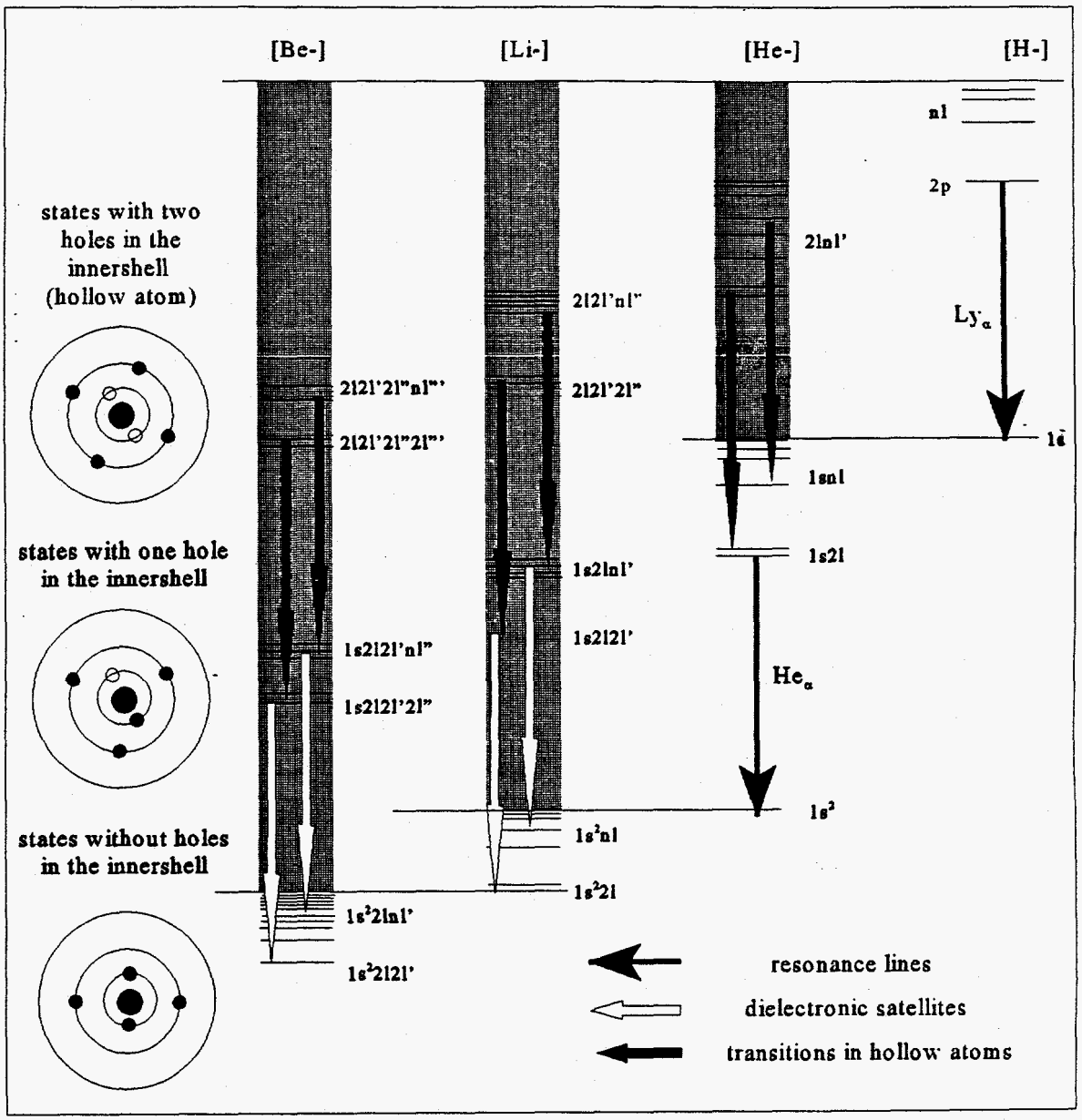

Fig.10. The scheme of single-, double- and triple- excited states of ions.

Comparing the present results with spectra obtained in the more usual case of nanosecond laser plasmas, i.e. plasma created by nanosecond laser pulses (see, for example, Skobelev et al[2]), we find:

1) when a plasma is created by a subnanosecond laser pulse that is much longer than few picoseconds ("subnanosecond plasma"), its emission spectra are very close to the spectra of nanosecond plasma,

2) the emission properties of "subpicosecond plasma" strongly depend on the contrast of laser pulse relative to any lower power laser prepulse - when the contrast is low (large prepulse) the spectra are, generally speaking, similar to the subnanosecond ones, while when the contrast is high ("no prepulse case") the plasma radiation has a more complex wavelength structure with a number of new spectral lines.

The collision-radiative kinetic models usually give a good description of radiative properties of nanosecond and subnanosecond laser plasma and allow the use of the observed spectra to measure some of the plasma parameters such as electron density and temperature[2]. These models also give satisfactory results for low- contrast subpicosecond plasma[5,14,15] , only if some additional physical processes are included into the kinetic calculations (for example: hot electrons, and or collisional excitation of autoionizing states from excited ones). However, the x-ray spectra of high-contrast subpicosecond plasma could not be explained in terms of commonly used theoretical models. The main discrepancy is that observed spectra show more complicated structures. This discrepancy can not be explained by only line broadening in a superdense plasma; a simple estimate, for the Ly_α line of an ion with Z=10 in a plasma with electron density $N_e=10^{24}$ cm^{-3} and electron temperature $T_e=100$ eV, gives a relative line width of $\Delta\lambda/\lambda=3\times10^{-4}$. This broadening is much smaller than the observed widths of the He- and H-like spectral lines.

The situation can be improved if the emission of lower charged ions than Li-like are taken into account. Figure 10 shows the energy levels that are responsible for the 2p-1s transitions in ions from H-like through Be-like one. The figure shoows that the usual dielectronic satellites structure of Ly_α and $He_{\alpha,\beta}$ lines can be enriched by the transitions from triply excited levels of Li- and Be-like ions ('hollow' ions) respectively. Such transitions have to be interpreted,or assigned, as the satellites for the resonance lines emitted by the ion of higher charge but multiple inners shell vacancies. This scheme can be continued to the left of Figure 10 and to the upper transitions from double *K*-vacancies levels (black arrow lines) and will give Ly_α hyper satellites while the lower (white arrow lines) from single *K*-vacancy levels side give $He_{\alpha,\beta}$ lines sattelites as well. Generally speaking the wavelengths would be longer but for lower-charge hyper satellites the 3p-1s transitions will match the assigned 2p-1s lines from the blue side. Thus detailed calculations are needed for the level structure of 'hollow' ions including energy positions and radiation probabilities. The other serious question is the mechanisms of population of 'hollow' ion levels perturbed by the environment. In the below surface region, the direct *K*-shell ionization seems to be the main channel of 'hollow' ion production. It is evident that the Auger transitions will play the significant role in the formation of ions and will affect their abundance.

REFERENCES

1. P. Gibbon, E. Forster, *Plasma Phys. Control. Fusion*, **38**, pp.769, 1996
2. I.Yu. Skobelev, A.Ya.Faenov, B.A. Bryunetkin et al, *JETP*, **108**, pp.1263, 1995
3. B.A. Bryunetkin, A.Ya. Faenov, V.M. Dyakin et al, *JQSRT*, **53**, pp.45, 1995
4. A.Ya. Faenov, I.Yu. Skobelev, S.A. Pikuz et al, *Phys. Rev.*, **A51**, pp.3529, 1995
5. F.B. Rosmej, B.A. Bryunetkin, A.Ya. Faenov et al, *J. Phys.*, **B29**, pp.L299, 1996
6. P. Audebert, J.P. Geindre, J.C. Gauthier et al, *Europhys. Lett.*, **19**, pp.189, 1992
7. P. Audebert, J.P. Geindre, A. Rouse et al, *J. Phys.*, **B27**, pp.3303, 1994
8. A. Zigler, V.Z. Jacobs, D.A. Newman et al, *Phys. Rev.*, **A45**, pp.1569, 1992
9. B.A. Bryunetkin, I.Yu. Skobelev, A.Ya. Faenov et al, *JETP Lett.*, **62**, pp.31, 1995
10. J.-P. Briand, G. Giardino, G. Borsoni. et. al. *Phys. Rev.*, **A54**, pp. 4136, 1996
11. S. Ninomiya, Y. Yamazaki, F. Koike, et. al. *Phys. Rev. Lett.*, **78**, pp.4557, 1997
12. U. Trumm, *Phys. Rev.*, **A55**, pp.478, 1997
13. I.Yu. Skobelev, A.Ya. Faenov, A.I. Magunov et al, *Physika Scripta*, 1997 (in press)
14. G. A. Kyrala, R. D. Fulton, et al, Appl. Phys. Letters, **60**, 2195 (1992).
15. J. Abdallah et al, *JQSRT*, 1998 (to be published)